ROR1 is essential for proper innervation of auditory hair cells and hearing in humans and mice

Oscar Diaz-Horta[a], Clemer Abad[a], Levent Sennaroglu[b], Joseph Foster II[a], Alexandra DeSmidt[c], Guney Bademci[a], Suna Tokgoz-Yilmaz[b], Duygu Duman[d], F. Basak Cengiz[d], M'hamed Grati[e], Suat Fitoz[f], Xue Z. Liu[e], Amjad Farooq[g], Faiqa Imtiaz[h,i], Benjamin B. Currall[h], Cynthia Casson Morton[h,j,k,l], Michiru Nishita[m], Yasuhiro Minami[m], Zhongmin Lu[c], Katherina Walz[a,n], and Mustafa Tekin[a,e,n,1]

[a]John P. Hussman Institute for Human Genomics, University of Miami Miller School of Medicine, Miami, FL 33136; [b]Department of Otolaryngology, Hacettepe University School of Medicine, Ankara, 06100, Turkey; [c]Department of Biology, University of Miami, Miami, FL 33146; [d]Division of Pediatric Genetics, Ankara University School of Medicine, Ankara, 06100, Turkey; [e]Department of Otolaryngology, Miller School of Medicine, University of Miami, Miami, FL 33136; [f]Department of Radiology, Ankara University School of Medicine, Ankara, 06100, Turkey; [g]Department of Biochemistry and Molecular Biology, Miller School of Medicine, University of Miami, Miami, FL 33136; [h]Department of Obstetrics, Gynecology and Reproductive Biology, Brigham and Women's Hospital and Harvard Medical School, Boston, MA 02115; [i]Department of Genetics, King Faisal Specialist Hospital & Research Centre, Riyadh 11211, Saudi Arabia; [j]Department of Pathology, Brigham and Women's Hospital and Harvard Medical School, Boston, MA 02115; [k]The Broad Institute of MIT and Harvard, Cambridge, MA 02142; [l]Manchester Academic Health Science Center, University of Manchester, Manchester M13 9NT, United Kingdom; [m]Department of Physiology and Cell Biology, Kobe University School of Medicine, Kobe, 650-0017, Japan; and [n]Dr. John T. Macdonald Foundation Department of Human Genetics, University of Miami Miller School of Medicine, Miami, FL 33136

Edited by Mary-Claire King, University of Washington, Seattle, WA, and approved April 19, 2016 (received for review November 16, 2015)

Hair cells of the inner ear, the mechanosensory receptors, convert sound waves into neural signals that are passed to the brain via the auditory nerve. Little is known about the molecular mechanisms that govern the development of hair cell–neuronal connections. We ascertained a family with autosomal recessive deafness associated with a common cavity inner ear malformation and auditory neuropathy. Via whole-exome sequencing, we identified a variant (c.2207G>C, p.R736T) in ROR1 (receptor tyrosine kinase-like orphan receptor 1), cosegregating with deafness in the family and absent in ethnicity-matched controls. ROR1 is a tyrosine kinase-like receptor localized at the plasma membrane. At the cellular level, the mutation prevents the protein from reaching the cellular membrane. In the presence of WNT5A, a known ROR1 ligand, the mutated ROR1 fails to activate NF-κB. *Ror1* is expressed in the inner ear during development at embryonic and postnatal stages. We demonstrate that *Ror1* mutant mice are severely deaf, with preserved otoacoustic emissions. Anatomically, mutant mice display malformed cochleae. Axons of spiral ganglion neurons show fasciculation defects. Type I neurons show impaired synapses with inner hair cells, and type II neurons display aberrant projections through the cochlear sensory epithelium. We conclude that *Ror1* is crucial for spiral ganglion neurons to innervate auditory hair cells. Impairment of *ROR1* function largely affects development of the inner ear and hearing in humans and mice.

deafness | whole-exome sequencing | inner ear | innervation | NF-κB

Sensorineural hearing loss (SNHL) is diagnosed in approximately 1 per 500 newborns (1). A genetic etiology is present in more than half of the cases. Inner ear anomalies (IEAs), demonstrated with computerized tomography or magnetic resonance imaging, are associated with SNHL in about one-third of individuals (2). Although IEAs can be diagnosed in patients with other clinical manifestations, such as those seen in Waardenburg [Mendelian Inheritance in Man (MIM) 193500], Pendred (MIM 274600), or BOR (MIM 113650) syndromes, the majority of cases fall into the category of nonsyndromic deafness. Despite recent progress in identifying genes that determine many forms of hearing loss (hereditaryhearingloss.org/), the genetic basis of IEAs in humans remains largely unknown.

The inner ear is a complex organ that is built from a simple structure, referred to as the otocyst, through a series of morphogenetic events. Roughly, it consists of a dorsal vestibular and a ventral auditory component (3). Studies in model organisms have identified a number of genes that play roles in proper development of the inner ear. Mouse models have been particularly relevant because the anatomy and physiology of the murine auditory system are similar to those of humans. Mutations in human orthologs of many of these genes have been reported to cause deafness in humans as well (4).

Next-generation sequencing technologies have allowed rapid identification of novel human deafness genes. Approximately 85% of disease-causing mutations in Mendelian disorders have been found in the protein-coding regions, despite the fact that this portion accounts for less than 2% of the entire human genome (5). Accordingly, whole exome sequencing (WES) has been frequently used because it allows for a targeted enrichment and resequencing of nearly all exons of protein-coding genes.

In this study, via WES, we detected a mutation in *ROR1* (receptor tyrosine kinase-like orphan receptor 1; MIM 602336), encoding receptor tyrosine kinase-like orphan receptor 1, that associates with an IEA and nonsyndromic deafness in a family. Further characterization of *Ror1* mutant mice revealed that *Ror1* deficiency results in defective hair cell innervation and abnormal cochlear development.

Results

A Missense Mutation in *ROR1* Causes an Inner Ear Anomaly and Profound Sensorineural Hearing Loss in a Turkish Family. In a consanguineous family of Turkish origin with two children having congenital profound SNHL (Fig. 1*A* and *SI Appendix*, Fig. S1*A*), high-resolution

Significance

The inner ear is a vertebrate organ of delicate and complex architecture that translates sound into electrical signals deciphered by the brain. This study utilizes a genetic approach to associate a mutation of *ROR1* (receptor tyrosine kinase-like orphan receptor 1) with inner ear anomalies and deafness in humans. Characterization of *Ror1* mutant mice reveals fasciculation deficiencies of spiral ganglion axons and disruption of sensory hair cell synapses and peripheral innervations. The molecular basis of this phenotype involves alterations of the NF-κB pathway. Thus, we present *ROR1* as a previously unrecognized gene that is essential for the development of the inner ear and hearing in humans and mice.

Author contributions: O.D.-H., K.W., and M.T. designed research; O.D.-H., C.A., L.S., J.F., A.D., G.B., D.D., F.B.C., M.G., A.F., F.I., B.B.C., C.C.M., M.N., Y.M., K.W., and M.T. performed research; O.D.-H., C.A., L.S., J.F., G.B., S.T.-Y., F.B.C., S.F., X.Z.L., A.F., C.C.M., M.N., Y.M., Z.L., K.W., and M.T. analyzed data; and O.D.-H., S.F., A.F., C.C.M., M.N., Y.M., K.W., and M.T. wrote the paper.

The authors declare no conflict of interest.

This article is a PNAS Direct Submission.

[1]To whom correspondence should be addressed. Email: mtekin@miami.edu.

This article contains supporting information online at www.pnas.org/lookup/suppl/doi:10.1073/pnas.1522512113/-/DCSupplemental.

GENETICS

computerized tomography scans of the temporal bone showed an inner ear anomaly consisting of fusion of the cochlea and vestibule into a common cavity (Fig. 1*B*). Distortion product otoacoustic emissions (DPOAEs) were present in the tested sibling (II:2), which is indicative of auditory neuropathy (*SI Appendix*, Fig. S1*B*). Patients did not show signs of impaired balance and had normal neuromotor development except for speech and language delay. Although one affected child (II:1) had unilateral iris coloboma and unilateral pseudo cleft lip, the other sibling had no additional abnormalities. Individual II:2 received a cochlear implant, which improved her hearing levels (*SI Appendix*, Fig. S1*A* and Table S1). Sequencing of the whole exome in individuals II:1 and II:2 generated a mean coverage of 58.6- and 58.9-fold, respectively; 94.7% and 95.1% of targeted reads had greater than twofold coverage, respectively. Filtering of DNA variants according to autosomal recessive inheritance (based on criteria given in *SI Appendix, Materials and Methods*) herein yielded one homozygous variant, chr1:64,643,931G>C (hg19), corresponding to *ROR1* c.2207G>C (NM_005012.3, GenBank), p.R736T.

In individuals II:1 and II:2, this variant was within a 6.9-Mb and 6.2-Mb region of homozygosity at chr1:59,156,137–66,067,396 and chr1:59,844,513–66,067,396, respectively. Affected individuals did not have a pathogenic variant in any other genes known to cause deafness. Also no pathogenic copy number variation was detected in affected individuals via SNP arrays. Sanger sequencing showed cosegregation with the phenotype in the family (Fig. 1 *A* and *C*). The variant was absent from public databases ExAC (exac.broadinstitute.org/), EVS (evs.gs.washington.edu/EVS/), and 1000 Genomes (www.1000genomes.org/) and was also absent in 330 Turkish controls. In silico analyses for pathogenicity [sorting intolerant from tolerant (SIFT) and PolyPhen-2 scores] were both deleterious: 0 and 1, respectively. Of 248 other autosomal recessive families and 437 simplex cases with nonsyndromic SNHL, no other individuals harbored mutations in *ROR1*.

Molecular modeling established by using the homologous ROR2 (receptor tyrosine kinase-like orphan receptor 2), a protein with a known crystal structure (PDB ID code 3ZZW), indicated that the mutated amino acid (p.R736T) localizes to the tyrosine kinase catalytic domain (*SI Appendix*, Fig. S2), leading to a conformational change that may impair substrate binding.

R736T Impairs the Plasma Membrane Subcellular Localization of ROR1, Enhances Ubiquitination, and Affects Downstream NF-κB Activation. Confocal microscopy of Madin–Darby canine kidney (MDCK II) cells transfected with a construct encoding WT *ROR1-GFP* showed that the protein is expressed in the plasma membrane (*SI Appendix*, Fig. S3 *A–E*) and colocalizes with another transmembrane protein, ROR2 (6). In contrast, the mutated ROR1-GFP was less represented in the plasma membrane (*SI Appendix*, Fig. S3 *A–E*).

Misfolded proteins compromise cellular function. How these proteins are detected and degraded is not well understood. However, ubiquitination followed by proteasome degradation has been described as one of the implicated mechanisms (7). Previous reports have shown that some proteins/enzymes become protected from ubiquitination upon substrate binding (8). Because our molecular modeling predicted that the mutation might affect ROR1 ATP binding (*SI Appendix*, Fig. S2), we aimed at determining whether the amino acid change triggers ubiquitination in overexpressing cells. *SI Appendix*, Fig. S4 shows that ubiquitination is enhanced in R736T ROR1, as a result of either misfolding or substrate protection.

Previous reports identified WNT5A (wingless-type MMTV integration site family, member 5a) as a ligand of ROR1 (9). Upon binding of WNT5A, ROR1 can activate NF-κB (nuclear factor kappa-B). Deficiency of NF-κB is associated with defective neuronal survival and hearing loss in mice (10). NF-κB signaling is also implicated in hippocampal neuron neurite outgrowth (11) (*SI Appendix*, Fig. S3*F*). Accordingly, we showed with firefly/*Renilla* luciferase luminescence ratios that ROR1 induces activation of NF-κB, an effect that is increased in cells overexpressing WNT5A. However, this effect is absent in cells overexpressing mutant ROR1 (*SI Appendix*, Fig. S3*G*).

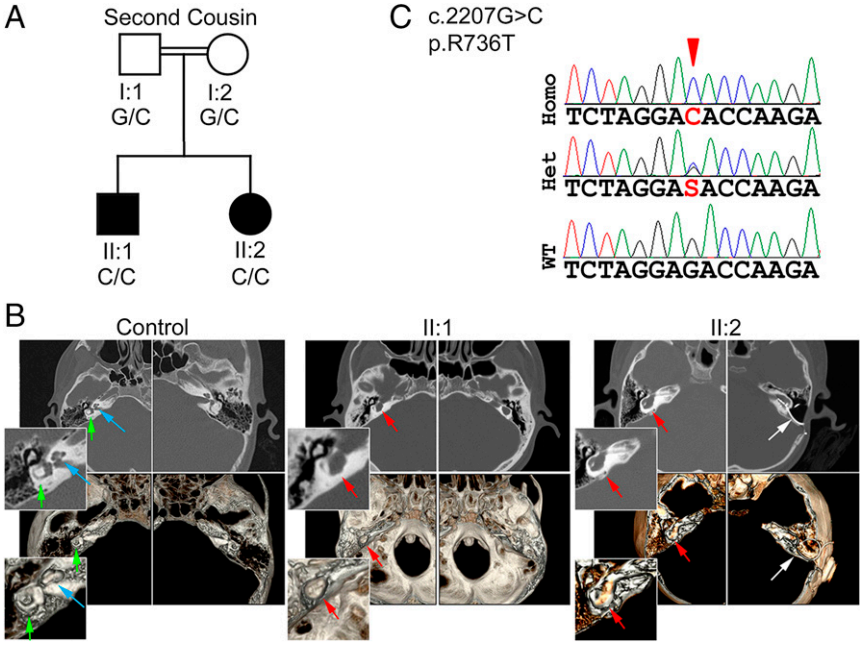

Fig. 1. Pedigree, *ROR1* mutation, and inner ear anomalies detected in the family. (*A*) Family of Turkish origin with congenital hearing loss (black symbols) and genotypes at *ROR1* c.2207G>C. The double bar indicates a consanguineous marriage. (*B*) Computed tomography scans [single horizontal planes (*Upper*) and 3D rendering (*Lower*)] showing the inner ear region in hearing and affected individuals as indicated on the top of each panel. Blue and green arrows indicate normal cochlea and vestibule, respectively. Red arrows indicate the common cavity present in affected individuals. White arrows point to the cochlear implant in individual II:2. (*C*) Electropherograms showing the identified mutation. The WT traces are from an unrelated individual.

Auditory Neuropathy and Inner Ear Anatomic Defects in Ror1 Mutant Mice. In this study, we used previously generated *Ror1* mutant mice (12). Briefly, the exon of the *Ror1* gene, containing an Ig-like domain, was replaced by the neo gene. This construct was inserted into the E14 line of embryonic stem cells by electroporation, and homologous recombinants were selected by G418 and ganciclovir (12). *Ror1* transcripts tested by RT-PCR using primers (*SI Appendix*, Table S2) designed to amplify *Ror1* exon 2 and 3 were absent in *Ror1* mutant mice (*SI Appendix*, Fig. S5*A*) (12). However, using primers (*SI Appendix*, Table S2) designed to amplify *Ror1* exon 1–6 in mouse embryonic fibroblast (MEF)-derived cDNA, we detected unexpectedly two *Ror1* transcripts in *Ror1* mutants: i.e., one transcript lacked exons 3 and 4 (variant 2), and another one lacked exon 3 (variant 1) (288 bp, corresponding to the 96 amino acid residues within the Ig-like domain of ROR1) (*SI Appendix*, Fig. S5). Although the former transcript possesses a very early termination codon due to a frame shift in exon 5, the latter transcript can produce a truncated ROR1 protein with a 96-aa deletion within its Ig-like domain (13). Similarly to MEFs, both variants were present in mutant mouse inner ears, with the shortest transcript more abundantly expressed (*SI Appendix*, Fig. S5*E*), suggesting that *Ror1* mutant mice might exhibit a hypomorphic phenotype rather than a complete null phenotype.

Auditory brain-stem response (ABR) tests record electrical signals resulting from neuronal activities associated with auditory information processing. This test has been proven to be effective for assessing auditory function in mice (14). Responses were recorded upon delivering sound stimuli with varying frequencies (click and 8–24 kHz) and intensities (20–100 dB) in both WT and *Ror1* mutant mice (8- to 12-wk-old mice). In *Ror1* mutant mice, ABR thresholds for the click and all tested frequencies (pure tones) were >70 dB, indicating severe deafness (Fig. 2*A* and *SI Appendix*, Fig. S6*C*).

Otoacoustic emissions (OAEs) are low level sounds originating in the cochlea due to mechanical activity of outer hair cells (OHCs) (15). Absent or impaired ABRs and the presence of OAEs are indicative of auditory neuropathy. We measured distortion product-evoked OAEs (DPOAEs) and ABRs in each mouse group during the same session. DPOAEs were present in all tested mice (defined as evoked distortion product intensities over the mean plus one SD of the background noise). However, amplitudes produced by the *Ror1* mutant were reduced (not completely abrogated) in low/mid frequencies but remained similar at the highest tested frequency (2f1 − f2 = 24 kHz) (Fig. 2*B*).

Ror1 mutant mouse inner ears were paint-filled and photographed to assess anomalies indicative of the human phenotype (16). Fig. 2*C* and *SI Appendix*, Fig. S6*D* show defects in mutant

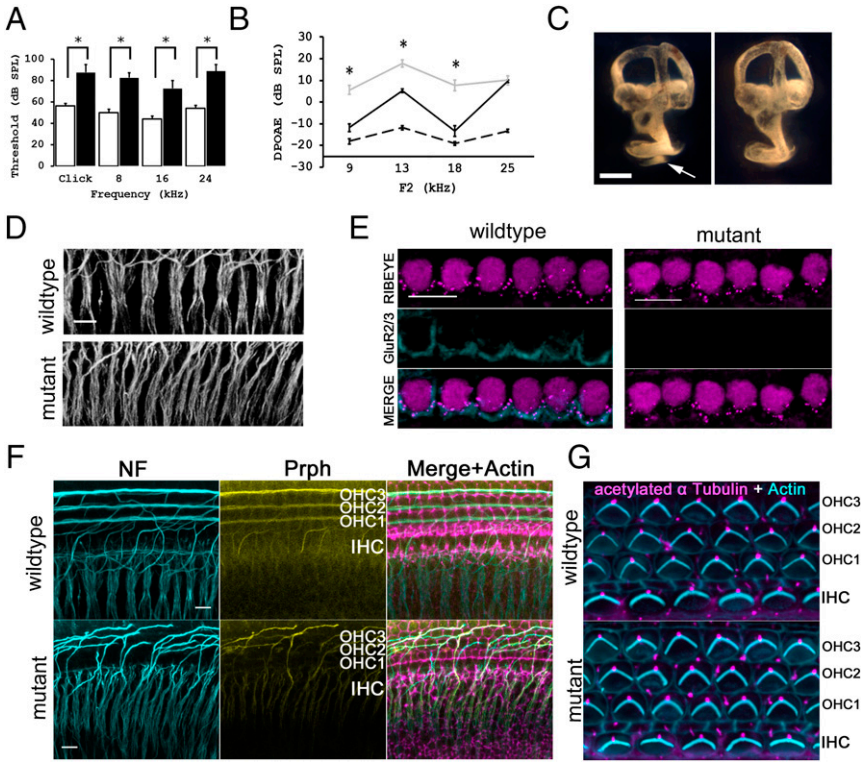

Fig. 2. Mouse model to study Ror1 function. (*A*) Eight- to 10-wk-old *Ror1* mutant mice show increased ABR thresholds ($n = 4$, black columns) in comparison with WT mice ($n = 5$, white columns). Values are represented as averages + SEM. *$P < 0.0005$. Two-way ANOVA and *t* test pairwise comparisons were performed to determine the statistical significance of differences. (*B*) Distortion product amplitudes for four frequencies (2f1 − f2) between 8 and 24 kHz in *Ror1* mutant (black line) and WT (gray line) mice. Noise floor is indicated with a dashed line. Values are represented as average ± SEM; *$P < 0.0005$. Two-way ANOVA and *t* test pairwise comparisons were performed to determine the statistical significance of differences. (*C*) Paint fills of the inner ear at P0 for WT (*Left*) and *Ror1* mutant (*Right*) mice. The arrow indicates a normal cochlear morphology. Note that *Ror1* mutant cochleae are smaller and under-coiled. (Scale bar: 500 μm.) (*D*) Representative *z*-stack projections showing radial bundle fibers with fasciculation defects in cochlea whole mount preparations from mutant Ror1 mouse. Nerve fibers are immunolabeled with an antibody against neurofilament heavy chain. (Scale bar: 10 μm.) (*E*) Representative *z*-stack projections obtained from P8 mice organ of Corti inner hair cells stained for anti-RIBEYE/CtBP2 (magenta) and GluR2/3 (cyan). Synaptic ribbons are identified as small RIBEYE-positive puncta. Anti-GluR2/3 signals indicate post-synaptic glutamate receptors that are not detectable in mutant mice preparations. (*F*) Total innervation pattern (*z*-stack images) of hair cells by SGN in the base of the cochlea of P5 WT and mutant whole-mount preparations. Immunolabeling for neurofilament heavy chain (NF) and peripherin (Prph) distinguishes type I and type II SGN innervation. Phalloidin was used for actin counterstaining (magenta). (Scale bar: 10 μm.) (*G*) Representative two-plane (apical plus basolateral) projections of inner ear hair cells showing normal stereociliary bundle orientation in P5 *Ror1* mutant cochlea. An acetylated α-tubulin antibody stains the hair cell kinocilium (magenta). Phalloidin (cyan) stains the hair cell bundle. The location of a single IHC and three OHC rows are indicated. (Scale bar: 10 μm.)

mice with under-coiled and shortened cochleae. The width of the organ of Corti did not seem to be affected (*SI Appendix*, Fig. S6*E*). There was an increase in hair cell density toward the apex, suggesting that the shortened cochlea was due to impaired convergent extension (*SI Appendix*, Fig. S6*F*). Vestibular anatomy was normal. Absence of any circling or balance defects and normal performance in the rotating rod test suggested normal vestibular function in *Ror1* mutant animals (*SI Appendix*, Fig. S6*B*).

Radial Bundle Fasciculation, Ribbon Synapse, and Innervation Pattern of Outer Hair Cells Are Disrupted in Ror1 Mutants. To investigate the effect of *Ror1* deficiency on the neuronal phenotype within the organ of Corti, we analyzed the total innervation pattern (*z*-stack images) in P5 whole-mount surface preparations of cochlea labeled with anti-neurofilament antibody and counterstained with phalloidin. In cochlear development, spiral ganglion neurons (SGNs) project peripheral axons through surrounding mesenchyme cells, forming dense fascicles before penetrating the sensory epithelium (17). Each bundle is formed of fibers with similar frequency tuning. This distinct fasciculation pattern is more evident at the base/mid region of the cochlea than at the apex (17). SGN axons in *Ror1* mutant cochlea failed to fasciculate correctly, arranging in less condensed bundles (Fig. 2*D*). To quantify fasciculation, we measured the total area occupied by SGN axons (*SI Appendix*, Fig. S6*G*) between the soma and the sensory epithelium as previously described (17).

Two types of afferent innervation extend into the cochlear epithelium: type I and type II spiral ganglion axons that connect with inner and outer hair cells, respectively. Type I SGNs constitute the vast majority of SGNs (~90%) and solely innervate the inner hair cells (IHCs). IHCs constitute the genuine sensory cells of the cochlea, which are functionally coupled to the OHCs, the cochlear amplifier. IHCs' synaptic active zones are equipped with a presynaptic electron-dense structure known as ribbon, to which synaptic vesicles are tethered. These structures can be visualized with an anti-RIBEYE antibody. Ribbon synapses are glutamatergic; thus, glutamate release in response to IHC stimulation drives the depolarization of type I SGNs upon binding to the AMPA receptors of their afferent boutons (18). The present study shows that, although presynaptic ribbons seem to be unaffected (Fig. 2*E* and *SI Appendix*, Fig. S6*H*), the postsynaptic glutamate receptors are not detectable (Fig. 2*E*) in *Ror1* mutant mice. Type II fibers invade the organ of Corti, turning toward the base and forming three uniform bundled tracks running parallel between the Deiters' cells. To distinguish between type I and type II fibers, we used an anti-peripherin antibody that selectively recognizes the latter (19). In *Ror1* mutant mice, the regular arrangement of type II innervation was impaired and a striking reduction of the density of axons was noticed throughout the organ of Corti (Fig. 2*F* and *SI Appendix*, Fig. S7*B*). In the apex, some axons aberrantly turned toward the apex in the mutant cochlea. The significance of the observed type II SGN defect for hearing loss in *Ror1* mutant mouse model remains to be determined, considering that $Prph^{(-/-)}$ mice (which lack type II SGN innervation) have baseline hearing thresholds indistinguishable from WT mice (20).

Planar polarity describes the coordinated polarization of cells or structures in the plane of a tissue. Development of this planar polarity is necessary for normal hearing because stereociliary bundles are sensitive to vibrations only in a single plane (21). Planar polarization is also required for convergent extension, a polarized cellular movement that occurs during neural tube closure and cochlear extension. WNT5A is an ROR1 ligand (9, 13), and, similar to our *Ror1* mutant mouse, *Wnt5a* knockout (KO) mice have a shortened cochlea (22) and, in addition, rotated stereociliary bundles (21, 22). To assess the bundle orientation, we stained the bundles with phalloidin, a selective toxin that tightly binds f-actin. An anti-acetylated-α-tubulin antibody was used to identify the kinocilium. Morphology and stereociliary bundle orientation was normal in the *Ror1* mutant mice (Fig. 2*G*).

Ror1 Is Expressed in SGNs and the Stria Vascularis During Development of the Mouse Inner Ear. Up-to-date, detailed expression of *Ror1* in the inner ear has not been documented. We conducted a temporal and spatial analysis of Ror1 protein expression using an Ror1-specific antibody, along with a neuronal marker (anti-neurofilament heavy chain) and an inner ear hair cell marker (Myo7a) (Fig. 3). At embryonic day (E)14.5, Ror1 was detectable in spiral ganglia and the cochlear epithelium (CE). Noticeably, the signal intensities were not homogeneous along the CE. At this stage, SGNs' axons have already projected through the CE, reaching the differentiating auditory hair cells (Fig. 3*A*). Ror1 is also expressed in the vestibule at this embryonic stage (*SI Appendix*, Fig. S8*A*). At E17.5, Ror1 signals gain intensity in SGN axon terminals adjacent to auditory hair cells (Fig. 3*B*, arrowheads). In the differentiating CE, Ror1 expression was intense in the stria vascularis (SV). At this stage, the hair cell differentiation marker Myo7a (red signals) revealed the typical arrangement of hair cells into three rows of OHCs and a row of IHCs. Reissner's membrane had already emerged as a well-defined structure. By postnatal day (P)0, Ror1 was expressed in spiral ganglia and SGN terminals. However, Ror1 expression in the SV weakened (Fig. 3*C*). Signals in the tectorial membrane were not specific because they appeared in mutant mice cochlea (*SI Appendix*, Fig. S8*B*). The expression of *Ror1* was not limited to the inner ear (*SI Appendix*, Fig. S9).

NF-κB Pathway in the Mutant Mouse Cochlea. Given that NF-κB activation is impaired in ROR1 R736T overexpressing cells, we investigated the expression of an array of 84 NF-κB pathway-associated genes in the mouse cochlea. Our expression data

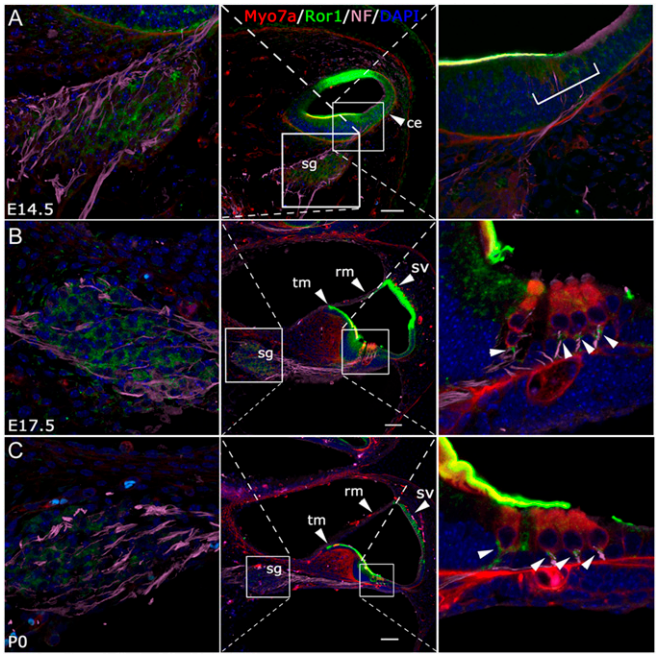

Fig. 3. Ror1 expression during development of the mouse cochlea. (*A*) At E14.5, Ror1 protein is expressed in the spiral ganglion (sg) and with heterogeneous intensity along cochlear epithelium (ce). At this stage, the differentiating organ of Corti (indicated with a bracket) is already invaded by SGN axons. For all images in *A*–*C*, *Middle*, the were recorded using a 20× objective lens. Areas enclosed in white squares were magnified with a 40× objective lens to visualize expression in detail (*Left* and *Right*). (*B*) At E17.5, Ror1 expression is intense in the developing stria vascularis (SV) and in SGN axon terminals (indicated with arrowheads). (*C*) At P0, Ror1 expression decays in SV but remains in SGN's terminals (arrowheads). The intensity of Ror1 signals in SGN's somas is similar during all three of the studied stages. (Scales bars: 50 μm.)

(*SI Appendix*, Table S3 and Fig. S10) showed that one gene, *Nfkbia*, is up-regulated in *Ror1* mutant cochleae. This protein actually inhibits NF-κB activation by sequestering its subunits in the cytosol (23). In turn, the down-regulated genes include (*i*) *Bcl3*, encoding for an atypical IκB protein family member, which acts as a nuclear transcriptional cofactor that associates with p50 and p52 homo- or heterodimers, subsequently promoting or suppressing downstream genes (24); (*ii*) *Birc3*, encoding for an apoptosis inhibitor (25); (*iii*) *Myd88*, encoding for a universal adapter protein used by almost all toll-like receptors (26); (*iv*) *Rela* and *Relb*, encoding for subunits of the NF-κB complex itself (24); (*v*) *Tlr9*, encoding a TLR family protein with a role in energy metabolism and cellular protection in neurons (27); and (*vi*) *Zap70*, encoding for a tyrosine kinase that promotes NF-κB activation through phosphorylation of Nfkbia (28).

Discussion

We identified *ROR1* as a gene involved in hearing using a genetic approach. This association was based on (*i*) identification of a homozygous mutation in a family with an inner ear anomaly and congenital deafness and (*ii*) detection of a cochlear malformation and severe deafness in *Ror1* mutant mice. Subsequent functional characterization allowed us to decipher a previously unidentified role for Ror1: the development of cochlear innervation. By recreating the human mutation (p.R736T), we showed that mutated ROR1 fails to reach the plasma membrane. This effect is suggested to be the result of enhanced ubiquitination. Mutated ROR1 failed to activate NF-κB irrespective of the presence of its ligand WNT5A (9).

ROR1 [previously known as neurotrophic tyrosine kinase, receptor-related 1 (*NTRKR1*)] is an integral transmembrane protein that consists of three extracellular conserved domains (Ig-like, frizzled, and kringle) and four intracellular domains (one tyrosine kinase, two serine/threonine-rich, and one proline-rich) (29). *Ror1* mutant mice exhibit a variety of phenotypic defects within skeletal and urogenital systems and display a postnatal growth retardation phenotype (12). The family presented here did not show syndromic findings, likely due to the fact that *ROR1*/*Ror1* mutations in humans and mice are different. There might be humans with syndromic findings associated with different mutations.

WNT5A has been described to bind the frizzled extracellular domain of ROR1, inducing the activation of transcription factor NF-κB (9). Wnt signaling has been shown to regulate planar cell polarity and convergent extension of cochlea in mice (21, 22). Particularly, *Wnt5a* knockout mice show misoriented stereocilia and a shortened cochlear duct (22). Our *Ror1* mutant mouse showed shortened cochleae (Fig. 2*C* and *SI Appendix*, Fig. S6*D*) but normal bundle orientation (Fig. 2*G* and *SI Appendix*, Fig. S7*A*), which is not a contradiction because dissociation of cochlear convergent extension and stereocilia orientation defects in some Wnt5a mutants suggest that the molecular mechanisms underlying these two processes are not identical (22). Previously, in situ hybridization experiments have shown *Wnt5a* expression in the cochlear epithelium during development (22). Because *Ror1* expresses in SGNs during all stages of development, we hypothesized that paracrine Wnt5a secretion may regulate Ror1-mediated SGN axon outgrowth. Coincidently, the onset and intensity of *Wnt5a* expression displays a basal-to-apical polarity along the longitudinal axis of the cochlear duct (22). The same polarity has been shown to be present by SGN axons in terms of density of individual fibers running between the Deiters' cells as well as the fasciculation degree of radial bundles crossing the otic mesenchyme (17).

WNT5A is a promiscuous ligand that has been shown to bind ROR2 (30), FZD5 (frizzled, drosophila, homolog of, 5) (31), and RYK (ryk receptor-like tyrosine kinase) (32), as well. In humans, mutations in *WNT5A* and *ROR2* cause autosomal dominant (MIM #180700) and recessive (MIM #268310) Robinow syndrome, respectively. The common features in both syndromes include the characteristic facial findings, skeletal abnormalities, and hypoplastic genitalia. Hearing loss is not a phenotypic finding in these syndromes. No human phenotype has been associated with mutations in *FZD5*, and the sole mutation documented for *RYK* has been linked to nonsyndromic cleft lip and palate.

Inhibition of NF-κB signaling has been shown to impair neurite outgrowth in cultured hippocampal neurons (11). NF-κB binding motifs predominate in promoter sequences of structural genes involved in synaptic remodeling (11). Ror1 and Ror2 are suggested as modulators of neurite extension in central neurons (33). NF-κB activation can be triggered by stimulation of a plethora of upstream receptors involved in the canonical, noncanonical, and atypical NF-κB pathways (34). There are no reports on deafness caused by the impairment of NF-κB signaling in humans. In mice, NF-κB deficiency has been shown to affect inner ear maintenance and/or regeneration (10), but not its development. NF-κB signaling defects have been linked to noise-induced auditory nerve degeneration (10) or chemical-driven hair cell death (35), but not congenital hearing loss. Here, we show that ∼10% of the investigated NF-κB pathway-associated genes are down-regulated whereas a cytoplasmic NF-κB inhibitor, *Nfkbia*, is up-regulated in mutant *Ror1* cochlea. It should be noted that only a small proportion of cells express Ror1 in the cochlea. Differences in NF-κB pathway-associated gene expression would be more striking if only those cells expressing Ror1 were analyzed. Altogether, the present study unveils ROR1 as a link between Wnt5a and the NF-κB pathway in the development of the murine inner ear.

Two lines of ideas have been proposed to explain how SGN's axon guidance is governed within the cochlea (36, 37). First is the release of chemo-attractants by the target epithelium and, more recently, the interaction of membrane receptors in neurons with repulsive factors along the path of peripheral axon outgrowth. Semaphorin3/Npn1, Eph/Ephrins, and Slit/Robo are typical receptor/ligand chemorepellent cognates expressed in the inner ear. In this study, we show that ROR1 deficiency impairs SGN radial bundle formation, a similar effect caused by mutations in other genes, such as *Pou3f4*, *Epha4*, and *Efnb2* (17, 37). Pou3f4 up-regulates the tyrosine kinase receptor Epha4 in the otic mesenchyme, which interacts with Efnb2 expressed on the surface of SGNs (17). It was proposed that Efnb2 may promote SGN axon–axon interaction via up-regulation of adhesion molecules or filopodial collapse (19). Similarly to the otic mesenchyme Epha4, SGN Ror1 is a tyrosine kinase receptor. Because Pou3f4/Epha4 signaling defects in the otic mesenchyme result in defective radial bundle formation, similarly, paracrine factors secreted by mesenchyme might be interacting with Ror1 in SGN. Alternatively, as aforementioned, Wnt5a secreted by the CE may exert a chemo-attractant effect regulating fasciculation. The other striking phenotypic defect in *Ror1* mutant cochlea is the impairment of synapses between IHC and type I SGN, as well as the pattern of type II innervation within the sensory epithelium. *Epha4* knockout mice show a reduction in the number of ribbon synapses, suggesting that fasciculation may directly impact target innervation (17). A knockout mouse for the R-spondin family, member 2 (Rspo2) displays similar disorganized fibers innervating outer hair cells (38). Remarkably, this protein is an activator of the canonical Wnt signaling pathway by acting as a ligand for LGR4-6 receptors. It will be important in future studies to investigate the details of Ror1-related SGN axon guidance.

Intriguingly, Ror1 is also expressed in the SV, an epithelial tissue in the lateral cochlear wall. The SV possesses a K^+ transport system that confers endolymph with unique electrochemical properties. In the SV, Ror1 expression is particularly high in early development; however, it decreases in late stages. The endocochlear potential generated by the SV starts to develop at P5 and progressively increases until adult age in mice (39). Thus, if there is a functional defect in the SV driven by mutant Ror1, it is unlikely to cause deafness because hair cell innervation is disrupted long before endocochlear potential is formed.

The impairment of ribbon synapses associated with *Ror1* deficiency clearly correlates with the increase of ABR thresholds and

conservation of OAEs in the mutant *Ror1* mice. Deafness and conserved OAE in the studied family indicated auditory neuropathy, suggesting that *ROR1* p.R736T mutation may also impair IHC innervation in humans. Auditory neuropathy is a nosological term conceived to describe hearing impairment originating downstream from mechanoelectrical transduction and cochlear amplification of OHCs (40). The known mechanisms of auditory neuropathy include dysfunction of inner hair cells, the SGN, and the ribbon synapse, also known as synaptopathy (40). Our study indicates that *ROR1* disruption leads to an auditory synaptopathy. Possibly, anatomical deformities of the inner ear detected in *Ror1* mutant mice and in humans are secondary to the neurological phenotype described herein. Potentially, these anomalies might be due to the pleiotropic effect of NF-κB deficiency (10).

In conclusion, we present *ROR1* as a deafness gene that associates with IEAs in humans. Likely, mutations in other genes in the same pathway would explain more cases with IEAs.

Materials and Methods

The study was approved by the Ethics Committee of Ankara University and the Institutional Review Board at the University of Miami. Informed consent was obtained from all participants. All animal handling and experimentation were performed in accordance with the University of Miami Institutional Animal Care and the National Research Council (US) *Guide for the Care and Use of Laboratory Animals* (41).

Human Genetic Studies. Whole-exome sequencing was performed using the genomic DNA of two affected individuals; after variant filtering, Sanger sequencing was performed to assess variant segregation with the phenotype; ROR1 structure was modeled based on homology with the known crystal structure of ROR2 (PDB ID code 3ZZW).

In Vitro Studies. WT and mutant ROR1 overexpressing cells were used to assess mutant ROR1 subcellular localization and ubiquitination; a firefly and *Renilla* luciferase reporter assay was used to investigate NF-κB activation.

Animal Studies. Hearing evaluation and characterization of the inner ear of an *Ror1* hypomorphic mutant mouse was performed.

Experimental methods are detailed in *SI Appendix*.

ACKNOWLEDGMENTS. We thank Jonathon Toft-Nielsen for technical assistance in performing hearing tests in mice; and Alexander Jacob Abrams, Matthew Condakes, and Katy Darvishi for assistance with data analysis. This study was supported by National Institutes of Health Grants R01DC012836 and R01DC009645 (to M.T.), R01GM083897 (to A.F.), R01DC012115 and R01DC05575 (to X.Z.L.), F32DC012466 (to B.B.C.), R01DC003402 (to C.C.M.), and R21DC009879; the University of Miami Provost Research Award and the College of Arts and Sciences Gabelli Fellowship (to Z.L.); a Harvard–Dubai Fellowship (to F.I.), and a SPARC grant from the Broad Institute (to C.C.M.).

1. Dror AA, Avraham KB (2009) Hearing loss: Mechanisms revealed by genetics and cell biology. *Annu Rev Genet* 43:411–437.
2. Sennaroglu L, Saatci I (2002) A new classification for cochleovestibular malformations. *Laryngoscope* 112(12):2230–2241.
3. Wu DK, Kelley MW (2012) Molecular mechanisms of inner ear development. *Cold Spring Harb Perspect Biol* 4(8):a008409.
4. Kikkawa Y, et al. (2012) Advantages of a mouse model for human hearing impairment. *Exp Anim* 61(2):85–98.
5. Botstein D, Risch N (2003) Discovering genotypes underlying human phenotypes: Past successes for mendelian disease, future approaches for complex disease. *Nat Genet* 33(Suppl):228–237.
6. Schwarzer W, Witte F, Rajab A, Mundlos S, Stricker S (2009) A gradient of ROR2 protein stability and membrane localization confers brachydactyly type B or Robinow syndrome phenotypes. *Hum Mol Genet* 18(21):4013–4021.
7. Kaganovich D, Kopito R, Frydman J (2008) Misfolded proteins partition between two distinct quality control compartments. *Nature* 454(7208):1088–1095.
8. Banerjee A, Kocarek TA, Novak RF (2000) Identification of a ubiquitination-target/substrate-interaction domain of cytochrome P-450 (CYP) 2E1. *Drug Metab Dispos* 28(2):118–124.
9. Fukuda T, et al. (2008) Antisera induced by infusions of autologous Ad-CD154-leukemia B cells identify ROR1 as an oncofetal antigen and receptor for Wnt5a. *Proc Natl Acad Sci USA* 105(8):3047–3052.
10. Lang H, et al. (2006) Nuclear factor kappaB deficiency is associated with auditory nerve degeneration and increased noise-induced hearing loss. *J Neurosci* 26(13):3541–3550.
11. O'Sullivan NC, Croydon L, McGettigan PA, Pickering M, Murphy KJ (2010) Hippocampal region-specific regulation of NF-kappaB may contribute to learning-associated synaptic reorganisation. *Brain Res Bull* 81(4-5):385–390.
12. Nomi M, et al. (2001) Loss of mRor1 enhances the heart and skeletal abnormalities in mRor2-deficient mice: Redundant and pleiotropic functions of mRor1 and mRor2 receptor tyrosine kinases. *Mol Cell Biol* 21(24):8329–8335.
13. Ho HY, et al. (2012) Wnt5a-Ror-Dishevelled signaling constitutes a core developmental pathway that controls tissue morphogenesis. *Proc Natl Acad Sci USA* 109(11):4044–4051.
14. Willott JF (2006) Overview of methods for assessing the mouse auditory system. *Curr Protoc Neurosci*, Chap 8, Unit 8.21A, pp 8.21A.1–8.21A.2.
15. Kemp DT (2002) Otoacoustic emissions, their origin in cochlear function, and use. *Br Med Bull* 63:223–241.
16. Morsli H, Choo D, Ryan A, Johnson R, Wu DK (1998) Development of the mouse inner ear and origin of its sensory organs. *J Neurosci* 18(9):3327–3335.
17. Coate TM, et al. (2012) Otic mesenchyme cells regulate spiral ganglion axon fasciculation through a Pou3f4/EphA4 signaling pathway. *Neuron* 73(1):49–63.
18. Safieddine S, El-Amraoui A, Petit C (2012) The auditory hair cell ribbon synapse: From assembly to function. *Annu Rev Neurosci* 35:509–528.
19. Barclay M, Ryan AF, Housley GD (2011) Type I vs type II spiral ganglion neurons exhibit differential survival and neuritogenesis during cochlear development. *Neural Dev* 6:33.
20. Froud KE, et al. (2015) Type II spiral ganglion afferent neurons drive medial olivocochlear reflex suppression of the cochlear amplifier. *Nat Commun* 6:7115.
21. Dabdoub A, et al. (2003) Wnt signaling mediates reorientation of outer hair cell stereociliary bundles in the mammalian cochlea. *Development* 130(11):2375–2384.
22. Qian D, et al. (2007) Wnt5a functions in planar cell polarity regulation in mice. *Dev Biol* 306(1):121–133.
23. Baeuerle PA, Baltimore D (1996) NF-kappa B: Ten years after. *Cell* 87(1):13–20.
24. Oeckinghaus A, Ghosh S (2009) The NF-kappaB family of transcription factors and its regulation. *Cold Spring Harb Perspect Biol* 1(4):a000034.
25. Pradhan M, Baumgarten SC, Bembinster LA, Frasor J (2012) CBP mediates NF-κB-dependent histone acetylation and estrogen receptor recruitment to an estrogen response element in the BIRC3 promoter. *Mol Cell Biol* 32(2):569–575.
26. Arancibia SA, et al. (2007) Toll-like receptors are key participants in innate immune responses. *Biol Res* 40(2):97–112.
27. Shintani Y, et al. (2013) TLR9 mediates cellular protection by modulating energy metabolism in cardiomyocytes and neurons. *Proc Natl Acad Sci USA* 110(13):5109–5114.
28. Livolsi A, Busuttil V, Imbert V, Abraham RT, Peyron JF (2001) Tyrosine phosphorylation-dependent activation of NF-kappa B. Requirement for p56 LCK and ZAP-70 protein tyrosine kinases. *Eur J Biochem* 268(5):1508–1515.
29. Borcherding N, Kusner D, Liu GH, Zhang W (2014) ROR1, an embryonic protein with an emerging role in cancer biology. *Protein Cell* 5(7):496–502.
30. Wallkamm V, et al. (2014) Live imaging of Xwnt5A-ROR2 complexes. *PLoS One* 9(10):e109428.
31. Blumenthal A, et al. (2006) The Wingless homolog WNT5A and its receptor Frizzled-5 regulate inflammatory responses of human mononuclear cells induced by microbial stimulation. *Blood* 108(3):965–973.
32. Andre P, et al. (2012) The Wnt coreceptor Ryk regulates Wnt/planar cell polarity by modulating the degradation of the core planar cell polarity component Vangl2. *J Biol Chem* 287(53):44518–44525.
33. Paganoni S, Bernstein J, Ferreira A (2010) Ror1-Ror2 complexes modulate synapse formation in hippocampal neurons. *Neuroscience* 165(4):1261–1274.
34. Gilmore TD (2006) Introduction to NF-kappaB: Players, pathways, perspectives. *Oncogene* 25(51):6680–6684.
35. Kim SJ, et al. (2015) Protective mechanism of Korean Red Ginseng in cisplatin-induced ototoxicity through attenuation of nuclear factor-κB and caspase-1 activation. *Mol Med Rep* 12(1):315–322.
36. Yang T, Kersigo J, Jahan I, Pan N, Fritzsch B (2011) The molecular basis of making spiral ganglion neurons and connecting them to hair cells of the organ of Corti. *Hear Res* 278(1-2):21–33.
37. Coate TM, Kelley MW (2013) Making connections in the inner ear: Recent insights into the development of spiral ganglion neurons and their connectivity with sensory hair cells. *Semin Cell Dev Biol* 24(5):460–469.
38. Mulvaney JF, et al. (2013) Secreted factor R-Spondin 2 is involved in refinement of patterning of the mammalian cochlea. *Dev Dyn* 242(2):179–188.
39. Sadanaga M, Morimitsu T (1995) Development of endocochlear potential and its negative component in mouse cochlea. *Hear Res* 89(1-2):155–161.
40. Moser T, Starr A (2016) Auditory neuropathy: Neural and synaptic mechanisms. *Nat Rev Neurol* 12(3):135–149.
41. National Research Council (US), Committee for the Update of the Guide for the Care and Use of Laboratory Animals, Institute for Laboratory Animal Research (US), & National Academies Press (US) (2011) *Guide for the Care and Use of Laboratory Animals* (National Academies Press, Washington, DC), 8th Ed, p xxv.